



## DESIGN AND REALIZATION OF AN ELECTRONIC CHARGE CONTROL CIRCUIT TO ATTENUATE THE HYSTERESIS OF THE HIGH RESOLUTION FABRY-PÉROT INTERFEROMETER'S AMPLIFIED PIEZOELECTRIC ACTUATORS

**Victor Atilio Marchiori**

**Fábio de Oliveira Fialho**

Laboratório de Automação e Controle – Departamento de Engenharia de Sistemas Eletrônicos da Escola Politécnica da Universidade de São Paulo – Avenida Professor Luciano Gualberto. Trv. 3, n° 158, São Paulo, Brazil

[victoratilio@usp.br](mailto:victoratilio@usp.br)

[fabio.fialho@usp.br](mailto:fabio.fialho@usp.br)

**Issa Ouattara**

Laboratoire d'Astrophysique de Marseille  
38, rue Frédéric Joliot-Curie, Marseille, France

[issa.ouattara@oamp.fr](mailto:issa.ouattara@oamp.fr)

**Ana Maria Molina Arcila**

Laboratório de Automação e Controle – Departamento de Engenharia de Sistemas Eletrônicos da Escola Politécnica da Universidade de São Paulo – Avenida Professor Luciano Gualberto. Trv. 3, n° 158, São Paulo, Brazil

[ammolina@usp.br](mailto:ammolina@usp.br)

**Fernando Moya Orsatti**

Laboratório de Automação e Controle – Departamento de Engenharia de Sistemas Eletrônicos da Escola Politécnica da Universidade de São Paulo – Avenida Professor Luciano Gualberto. Trv. 3, n° 158, São Paulo, Brazil

[fernando.orsatti@oepe.com.br](mailto:fernando.orsatti@oepe.com.br)

**Jair Pereira de Souza**

Laboratório de Microeletrônica – Departamento de Engenharia de Sistemas Eletrônicos da Escola Politécnica da Universidade de São Paulo – Avenida Professor Luciano Gualberto. Trv. 3, n° 158, São Paulo, Brasil

[jpsouza@lme.usp.br](mailto:jpsouza@lme.usp.br)

**Claudia Lúcia Mendes de Oliveira**

Instituto de Astronomia, Geofísica e Ciências Atmosféricas da Universidade de São Paulo  
Rua do Matão, n° 1226, São Paulo, Brazil

[oliveira@astro.iag.usp.br](mailto:oliveira@astro.iag.usp.br)

**Abstract.** *This paper presents the design and the realization of a technique to attenuate the hysteresis nonlinear phenomenon of high displacement Amplified Piezoelectric Actuators (APA) mounted in a state-of-the-art Fabry-Pérot interferometer. This interferometer is to be installed in the 3D-spectrometer Brazilian Tunable Filter Imager (BTFI) on the Southern Astrophysical Research (SOAR) telescope in Chile. The hysteresis attenuation technique presented in this paper aims to assist the Fabry-Pérot's nan positioning control system to attain its main scientific specification. In such system, each APA has a maximum stroke of  $270\mu\text{m}$  within a  $170\text{V}$  range, and they are used to position a high reflective mirror plate. The Fabry-Pérot's nan positioning control system is specified to limit the APA's positioning steady-state noise to  $3\text{nm rms}$ , but the hysteresis limits the positioning accuracy. In order to attenuate hysteresis, an electronic charge control circuit built with a high power operational amplifier has been designed and applied for each APA. The experiments results show that the hysteresis effect has almost been eliminated, and consequently the positioning steady-state noise has significantly been reduced.*

**Keywords:** *Piezoelectric Actuator, Hysteresis, Charge Control, Nan positioning Systems, Fabry-Pérot Interferometer*

V. A. Marchiori;F. O. Fialho;I. Ouattara

Design And Realization Of Electronic Charge Control System For Attenuating Hysteresis

## 1. INTRODUCTION

The Brazilian Tunable Filter Imager (BTFI) is a highly versatile, new technology, tunable optical imager to be used both in seeing-limited mode and at higher spatial fidelity using the SAM Ground-Layer Adaptive Optics facility (SOAR Adaptive Module) which is being deployed at the Southern Astrophysical Research (SOAR) telescope. The BTFI employs Fabry-Pérot interferometers in order to achieve high spectral resolutions up to  $R \sim 30,000$  (de Oliveira), as well as the use of an innovating technique of combining holographic nets to build a tunable filter. BTFI will be useful for the study of a variety of topics, from solar system bodies, stars, interstellar medium, galaxies, to cosmology.

The BTFI's Fabry-Pérot interferometer (Fig. 1a), or etalon, is an instrument that permits optical filtration by interference processes (Fig. 1d), given by multiple reflection and refraction of light between two parallel highly reflective surfaces (Fig. 1b). The refracted rays interfere on each other, forming a pattern which takes the appearance of a set of concentric rings (Fig. 1e). By tuning the distance between the parallel plates one tune the wavelength of light. In Fabry-Pérot interferometer, the distance between the parallel surfaces is controlled by Amplified Piezoelectric Actuators – APA – CEDRAT TECHNOLOGIES (Fig. 1c), which are fixed on the inner side of the etalon.

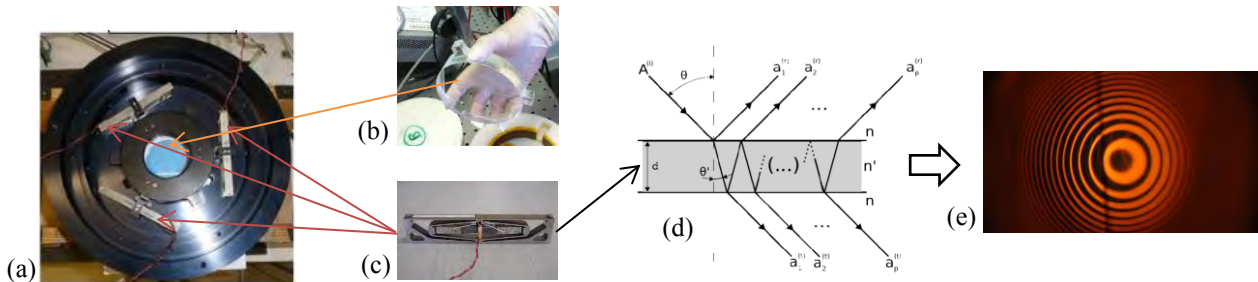


Figure 1. (a) Fabry-Pérot interferometer. (b) Mirror plate. (c) APA. (d) Interference process. (e) Visual pattern of concentric rings in Fabry-Pérot interferometer.

APA is a solid-state long-stroke actuator. It is based on the expansion of the active material and on a mechanism to amplify the displacement, which is also proportional to the applied voltage. The advantages of APA (Cedrat Technologies) are its relatively large displacements combined with its high forces and compact size along the active axis. Since APA is robust, it can also be used in dynamic applications, including in resonant devices. On the other hand, APA has a very typical type of nonlinearity encountered in piezoelectric transducers – the hysteresis – which limits the positioning accuracy.

Such non linearity, which appears when the piezoelectric transducers are submitted to conventional voltage control, is enormously undesirable for the Fabry-Pérot's nanopositioning system, since its main scientific specification imposes that the standard deviation of the positioning error must be limited to  $3nm$  rms. Thus, in order to attenuate the hysteresis effect of each APA in Fabry-Pérot, an analog charge control circuit built with a high power operational amplifier has been designed and applied for each APA. This paper aims to present the design and the implementation of such a solution, and to show its benefits by comparing the performance of the Fabry-Pérot's nanopositioning system with and without hysteresis attenuation.

Other techniques to attenuate the hysteresis have been widely published in other papers (Bazghaleh M., Beck J., Huang L., Rodriguez-Fortun J.M., Vautier B.J.G.). However, they are mostly limited to evaluate the results only in terms of the hysteresis magnitude reduction, without analyzing its improvements on a positioning accuracy point of view. With a more comprehensive approach, this paper focuses the analysis of the hysteresis attenuation in terms of the positioning accuracy of a real and challenging positioning application, giving an interesting contribution on this subject.

This paper is organized as follows: Section 2 describes the main characteristics of the Fabry-Pérot nanopositioning system's parts, Section 3 presents the method used to characterize the APA's hysteresis magnitude, Section 4 presents the charge control technique used to attenuate the APA's hysteresis and Section 5 presents the results obtained with the experiments performed with the APAs for both the classic voltage control (no hysteresis attenuation) and the designed charge control solutions. Finally, the experiment results are discussed in Section 6.

22nd International Congress of Mechanical Engineering (COBEM 2013)  
November 3-7, 2013, Ribeirão Preto, SP, Brazil

## 2. FABRY-PÉROT'S NANOPositionING SYSTEM

The actuating system of the Fabry-Pérot's nanopositioning system is composed by three APA400MML model (CEDRAT Technologies) Amplified Piezoelectric Actuators (APA).

The APA400MML (Fig. 2a) has a maximum stroke of  $270\mu\text{m}$  ( $-50\mu\text{m}$  to  $210\mu\text{m}$ ) and it is proportional to the applied voltage within a 170V range ( $-20\text{V}$  to  $+150\text{V}$ ). The APA400MML has two different excitation conditions: the quasistatic and the dynamic ones. The quasistatic excitation condition corresponds to operations in frequencies up to one-third of the first resonance frequency of the APA, which is about 600Hz. The dynamic excitation condition corresponds to operations in frequencies over the quasistatic bandwidth, in which the displacement becomes up to ten times more sensitive to the applied voltage than in quasistatic condition. Under an electronic point of view, each APA has an equivalent capacitance value of about  $10\mu\text{F}$ , which is valid in the quasistatic excitation condition.

The measuring system of the Fabry-Pérot's nanopositioning system is composed by three capacitive sensors and one converter module. Each capacitive sensor (Fig. 2b) have a measurement range of 1mm and a resolution of  $0,4\text{ nm RMS } \sqrt{\text{Hz}}$ . The converter module (Fig. 2c), which converts the signal coming from the capacitive sensors to a voltage signal, has a bandwidth of 10kHz and a maximum noise measure that is shorter than 0,005% RMS of the measure extent.



Figure 2. (a) Amplified Piezoelectric Actuator – APA. (b) Capacitive sensor. (c) Converter module.

## 3. HYSTERESIS CURVE CHARACTERIZATION

In general terms, the hysteresis on a dynamic system is a nonlinear phenomenon which presents a lag in response. In piezoelectric materials, this lag occurs between its displacement and the applied voltage. In other words, the displacement may assume different values for the same applied voltage. Like any other piezoelectric device, the Fabry-Pérot's APAs have this nonlinear characteristic, which limits the accuracy in positioning applications.

A graphical representation of the APA's displacement hysteresis is presented in Fig. 3. The hysteresis curve is partitioned into an ascending and into a descending branch, since the displacement trajectory depends on the sense of variation of the input voltage.

The calculation of the hysteresis magnitude (Agnus, J., 2003) is shown in Eq. (1):

$$H = \frac{(\delta_1 - \delta_2)}{(\delta_{\max} - \delta_{\min})} \times 100 \quad (1)$$

$H$  is the percentage hysteresis magnitude,  $(\delta_1 - \delta_2)$  is the maximum displacement difference between the ascending and the descending branches of the hysteresis curve for a same input voltage value, and  $(\delta_{\max} - \delta_{\min})$  is the difference between the displacement values at the maximum and the minimum applied voltages.

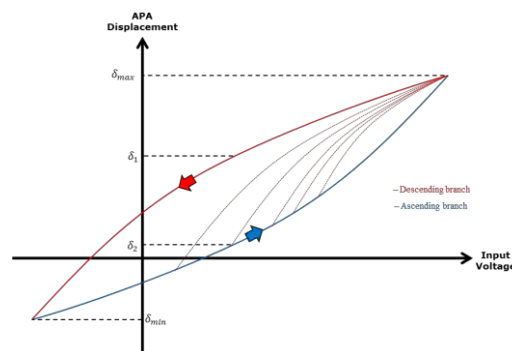


Figure 3. Hysteresis behavior of APA

V. A. Marchiori;F. O. Fialho;I. Ouattara  
Design And Realization Of Electronic Charge Control System For Attenuating Hysteresis

The dashed ascending branches in Fig. 3 illustrate the variation on the hysteresis curve as the minimum input voltage level is increased. It is possible to note that the terms  $(\delta_1 - \delta_2)$  and  $(\delta_{\max} - \delta_{\min})$  depend on the maximum and minimum values of the input voltage being applied, so the hysteresis magnitude will therefore depend on the maximum and minimum values of the input voltage.

#### 4. THE ANALOG CHARGE CONTROL SOLUTION

The charge control technique used in this paper lies on the principle that the displacement of a piezoelectric material is linearly proportional to the applied charge on it (Perez, R.). The electronic scheme shown in Fig. 4 presents one possible implementation of an analog charge control circuit.

In the scheme shown in Fig. 4, an APA with an inherent capacitance  $C_{pzt}$  is connected to the output and to the negative input of an operational amplifier (OA). This APA is also connected to a reference capacitor  $C_{ref}$  linked to the circuit ground. The input voltage signal is connected to the positive input of the operational amplifier.

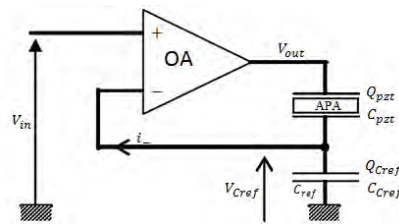


Figure 4. Charge Control solution (Comstock R.H.)

Let  $V_-$  be the voltage at the negative input of the operational amplifier and  $V_{in}$  be the input voltage signal. In that configuration, the current  $i_-$  across the negative input of the operational amplifier is on the order of micro amperes, which implies that the voltage  $V_{Cref}$  across the reference capacitor is practically equal to the voltage  $V_+$  at the positive input of the operational amplifier. In other words,  $V_{Cref}$  is such that:

$$V_{Cref} = V_- = V_+ = V_{in} \quad (2)$$

Moreover, it also implies that the charge  $Q_{pzt}$  across the APA is practically equal to charge  $Q_{Cref}$  across the reference capacitor, which is given by the expression in Eq. (4):

$$Q_{pzt} = Q_{Cref} \quad (3)$$

$$Q_{Cref} = C_{Cref} \times V_{Cref} = C_{Cref} \times V_{in} \quad (4)$$

$C_{Cref}$  is the capacitance value of the reference capacitor  $C_{ref}$ . Combining Eq. (3) and Eq. (4), the charge  $Q_{pzt}$  across the APA is given by the expression in Eq. (5):

$$Q_{pzt} = Q_{Cref} = C_{Cref} \times V_{in} \quad (5)$$

Therefore, the charge  $Q_{pzt}$  across the APA is proportional to the input voltage signal  $V_{in}$ . Since the APA's displacement is linearly proportional to applied charge  $Q_{pzt}$ , it implies that the APA's displacement will be linearly proportional to the input voltage signal  $V_{in}$ .

It is possible to show that the circuit gain, which is the relation between  $V_{out}$  and  $V_{in}$ , is approximately given by the expression in Eq. (6) (Agnes, J., 2003).

$$\frac{V_{out}}{V_{in}} = \frac{C_{Cref} + C_{pzt}}{C_{pzt}} \quad (6)$$

22nd International Congress of Mechanical Engineering (COBEM 2013)  
November 3-7, 2013, Ribeirão Preto, SP, Brazil

## 5. EXPERIMENTAL PROCEDURES

In order to obtain the APA's hysteresis curves and hysteresis magnitudes for both voltage and charge control configurations, according to the characterization method described in Section 3, the experiments shown in Fig. 5 have been set up.

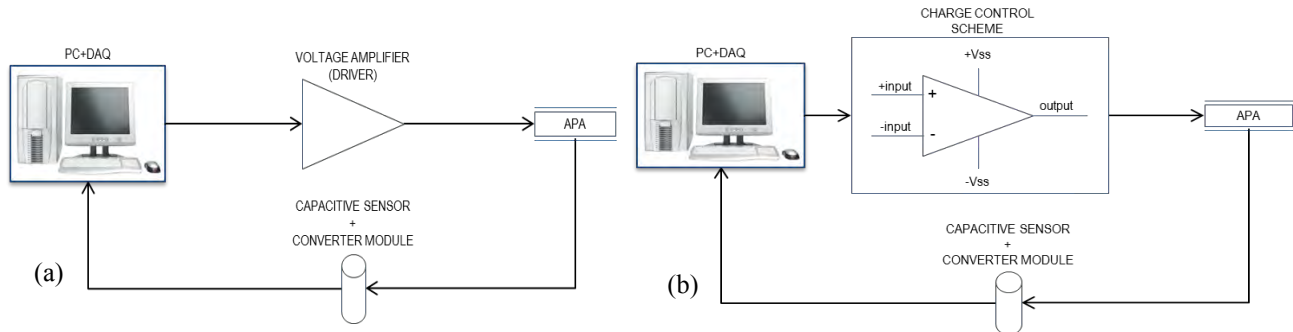


Figure 5. (a) Experiment scheme for determining the APA's hysteresis magnitude under voltage control. (b) Experiment scheme for determining the APA's hysteresis magnitude under charge control.

In these experiments, the PC runs simulation software which supports real-time communication with the data acquisition board (DAQ) connected to it. The DAQ provides a DC voltage signal varying from  $-10\text{V}$  to  $+10\text{V}$ , which supplies a voltage amplifier – driver (Fig. 5a) for voltage control configuration or an operational amplifier (Fig. 5b) for charge control configuration according to the scheme shown in Fig. 4. The driver has a fixed voltage gain which permits the APA to be supplied within its full voltage range ( $-20\text{V}$  to  $+150\text{V}$ ). For the charge control configuration, a high power operational amplifier was applied, which is also capable to deliver the full voltage range of the APA. The gain of the charge control circuit can be tuned by varying the value of  $C_{Cref}$ , as shown by Eq. (6).

The capacitive sensor and the capacitance to voltage converter described in Section 2 are used to measure the APA's displacement, which value is acquired by the PC software through an analog input of the DAQ.

### 5.1 Obtaining the hysteresis curves

In order to obtain the hysteresis curves of each piezo (APA) under voltage control configuration (Fig. 5a), a ramp voltage signal varying from  $-1\text{V}$  to  $+7.5\text{V}$  was generated in the PC software. A single cycle of this signal was transmitted directly to the driver input. Since the driver's voltage gain is 20, each piezo was supplied with a voltage signal varying from  $-20\text{V}$  to  $+150\text{V}$ . It allowed the piezos to achieve its full stroke of  $270\mu\text{m}$ .

In order to obtain the hysteresis curves of each piezo under charge control configuration (Fig. 5b), a ramp voltage signal varying from  $-1\text{V}$  to  $+7.5\text{V}$  was generated in the PC software. A single cycle of this signal was transmitted directly to the circuit input. In this experiment, the charge control circuit's voltage gain was set at approximately 20, therefore supplying each piezo with a voltage signal varying from about  $-20\text{V}$  to about  $+150\text{V}$ . It allowed the piezos to achieve its full stroke of  $270\mu\text{m}$ .

Figure 6 and Fig. 7 show the hysteresis curves obtained for the three piezos (Piezo A, B and C) under voltage and charge control, respectively.

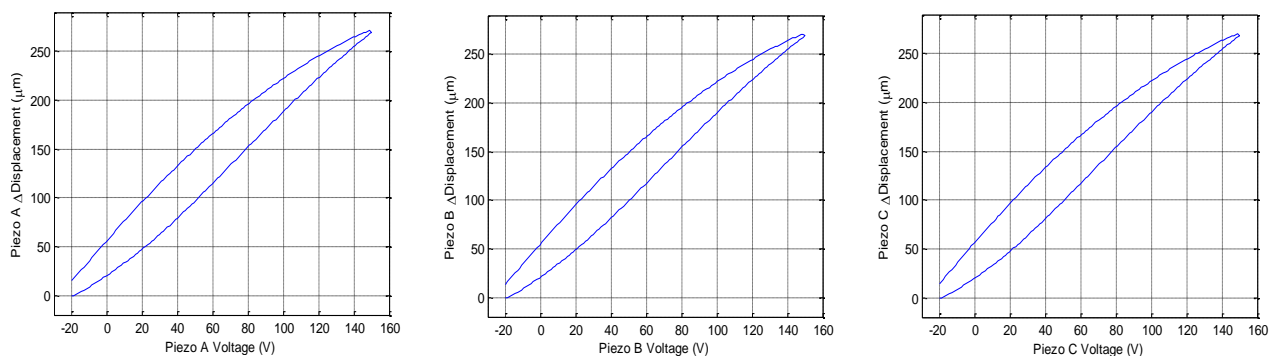


Figure 6. Hysteresis curves obtained for the piezos A (left), B (middle) and C (right) under voltage control.

V. A. Marchiori;F. O. Fialho;I. Ouattara

Design And Realization Of Electronic Charge Control System For Attenuating Hysteresis

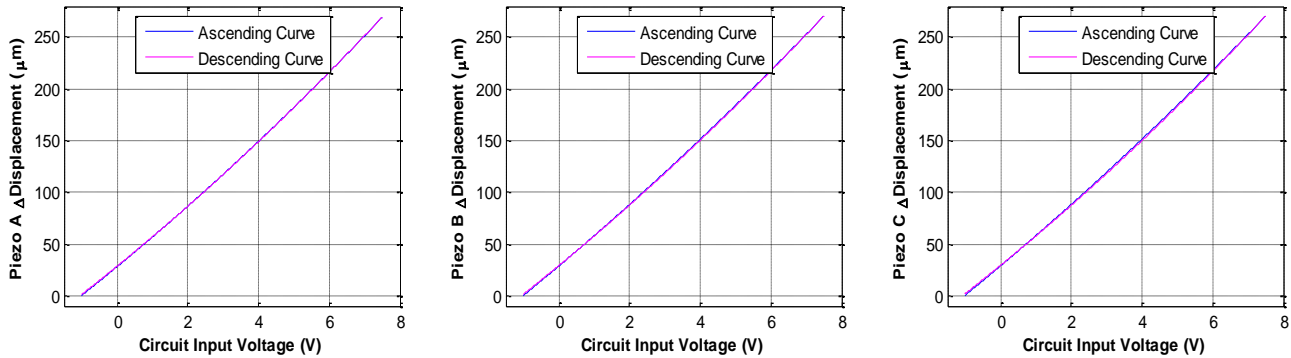


Figure 7. Hysteresis curves obtained for the piezos A (left), B (middle) and C (right) under charge control

Table 1 presents a resume of the results shown from Fig. 6 and Fig. 7 in terms of the hysteresis magnitude of the piezos.

Table 1. Comparative of the experimental results obtained for the hysteresis magnitude, according to Eq. (1), with the voltage control scheme (Fig. 5a) and the charge control scheme (Fig. 5b)

Piezo	Parameter	Voltage Control configuration	Charge Control configuration	Attenuation
A	Hysteresis Magnitude	19,9 %	0,35 %	98,2 %
B	Hysteresis Magnitude	18,7 %	0,47 %	97,5 %
C	Hysteresis Magnitude	19,5 %	0,63 %	96,8%

## 5.2 Evaluation of hysteresis attenuation in Closed Loop

In section 5.2, it was shown the benefits of using the analog charge control solution for attenuating the hysteresis magnitude. Nevertheless, in terms of nanopositioning, which is the subject of interest of this paper, the hysteresis magnitude does not give the real measure of the advantages that can be obtained by using such a solution.

Thus, additional experiments were performed in order to evaluate more directly the gains it brought for the Fabry-Pérot's nanopositioning system. To do such evaluation, the voltage control scheme of Fig. 5a and the charge control scheme of Fig. 5b were both set up in a closed-loop configuration, which was built with a digital PI compensator implemented within the simulation software running in the PC environment.

In such configuration (Fig. 8), the measured APA displacement signal  $y(t)$  is compared to a reference (set-point) signal  $r(t)$  in microns, whose error  $e(t)$  is processed by the PI compensator ( $K$ ) which generates a voltage control signal  $u(t)$  (control effort) limited within a -10V to +10V range. The control signal is transmitted to the system ( $G$ ) through the analog output of the DAQ. In voltage control configuration,  $G$  is the APA itself, while in charge control configuration  $G$  is the charge control circuit and the APA.

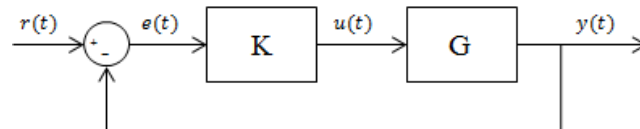


Figure 8. Closed-Loop configuration

For both voltage and charge control configurations, the PI compensator was manually tuned in order to provide the shorter response time possible without destabilizing the closed-loop system.

Figure 9 and Fig. 10 show the results obtained with the voltage control scheme (Fig. 5a) and the charge control scheme (Fig. 5b) submitted both to a closed-loop configuration. In Fig. 9, the control effort  $u(t)$  is evaluated under voltage and charge control configurations for the three piezos, while in Fig. 10 the measured displacement signal  $y(t)$  is evaluated under voltage and charge control configurations for the three piezos.

22nd International Congress of Mechanical Engineering (COBEM 2013)  
November 3-7, 2013, Ribeirão Preto, SP, Brazil

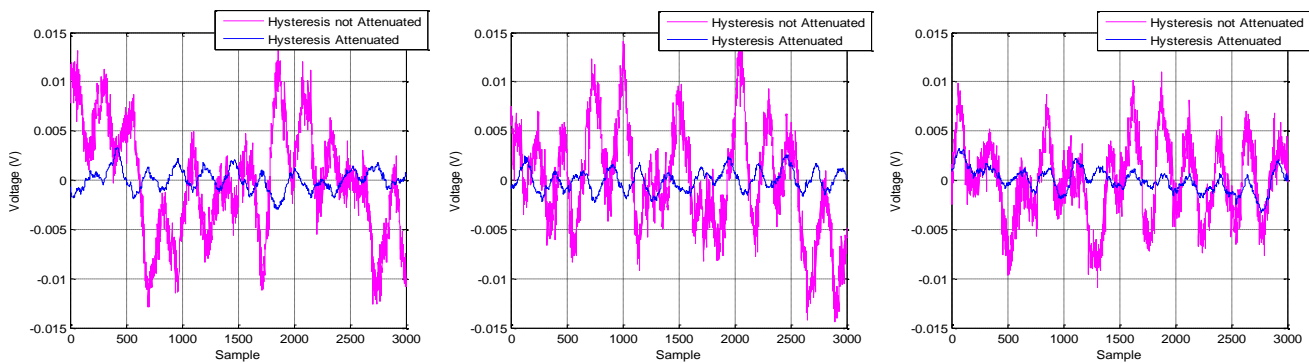


Figure 9. Control effort signals of the piezos A (left), B (middle) and C (right) obtained under voltage control (Hysteresis not Attenuated) and charge control (Hysteresis Attenuated) configurations in closed loop.

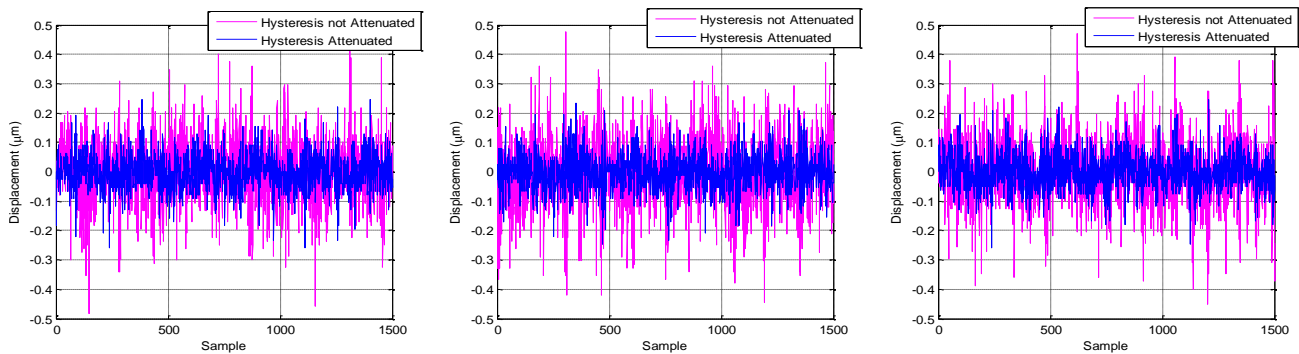


Figure 10. Displacement signals of the piezos A (left), B (middle) and C (right) obtained under voltage control (Hysteresis not Attenuated) and charge control (Hysteresis Attenuated) configurations in closed loop.

Table 2 presents a resume of the results shown from Fig. 9 and Fig. 10 in terms of the standard deviation of the control effort and the positioning error for each of the piezos.

Table 2. Comparative of the experimental results obtained for the control effort and the positioning error with the voltage control scheme (Fig. 5a) and the charge control scheme (Fig. 5b) submitted to a closed-loop configuration

Piezo	Parameter	Voltage Control configuration	Charge Control configuration	Attenuation
A	Control Effort's Standard Deviation	5,6 mV	1,1 mV	80,4%
	Positioning Error's Standard Deviation	108 nm	61 nm	43,5%
B	Control Effort's Standard Deviation	5,4 mV	2 mV	72,2%
	Positioning Error's Standard Deviation	122 nm	61 nm	50,0%
C	Control Effort's Standard Deviation	3,9 mV	1,2 mV	69,2%
	Positioning Error's Standard Deviation	133 nm	59 nm	55,6%

## 6. CONCLUSION

This paper describes the design and the realization of an analog charge control solution to attenuate the hysteresis nonlinear phenomenon of the Fabry-Pérot interferometer's Amplified Piezoelectric Actuators (APA). With the use of such system, the hysteresis magnitude is almost eliminated (up to 98,2% reduction) compared to the classic voltage control solution. Moreover, in order to verify the direct benefits of attenuating the hysteresis in positioning applications, the behavior of the charge control system is also evaluated in closed-loop. In such experiment, the standard deviations of the control effort and positioning error have significantly been reduced (up to 80,3% and up to 55,6% reduction respectively) compared to the voltage control solution.

## 7. ACKNOWLEDGEMENTS

V. A. Marchiori;F. O. Fialho;I. Ouattara

Design And Realization Of Electronic Charge Control System For Attenuating Hysteresis

## 8. REFERENCES

- Agnus, J., 2003. "Contribution à la micromanipulation. Etude, Réalisation, Caractérisation et Commande d'une Micropince Piézoélectrique". Thesis, Laboratoire d'Automatique de Besançon, Besançon.  
<[http://tel.archives-ouvertes.fr/docs/00/36/68/08/PDF/Joel\\_Agnus.pdf](http://tel.archives-ouvertes.fr/docs/00/36/68/08/PDF/Joel_Agnus.pdf)>.
- Bazghaleh M., Grainger S., Cazzolato B., Lu T. "An innovative digital charge amplifier to reduce hysteresis in piezoelectric actuators". School of Mechanical Engineering, The University of Adelaide, SA 5005, Australia.  
<<http://www.araa.asn.au/acra/acra2010/papers/pap111s1-file1.pdf>>.
- Beck, J., Noras M., Kieres J., E. Speich J. "Hysteresis characterization using charge feedback control for a LIPCA device," in *Smart Structures and Materials*, 2006, p. 61701M–61701M.
- de Oliveira, Cláudia Mendes, et al. "The Brazilian Tunable Filter Imager for the SOAR Telescope." *Publications of the Astronomical Society of the Pacific* 125.926 (2013): 396-408.
- Cedrat Technologies. *Products Catalogue* Version 4.1.  
<[http://www.cedrat-technologies.com/download/CEDRAT\\_TEC\\_Catalogue.pdf](http://www.cedrat-technologies.com/download/CEDRAT_TEC_Catalogue.pdf)>
- Comstock R.H., 1981. "Charge control of piezoelectric actuators to reduce hysteresis effects". *United States Patent* n° US 4,263,527 <<http://www.freepatentsonline.com/4263527.pdf>>
- Huang L., Ma Y.T., Feng Z. H., Kong F.R., 2010. "Switched capacitor charge pump reduces hysteresis of piezoelectric actuators over a large frequency range," *Review of Scientific Instruments*, vol. 81, no. 9, pp. 094701–094701, 2010.
- Perez, R., Agnus, J., Breguet, J.M., Chaillet, N., Bleuler, H., Clavel R., 2001. "Characterization and control of a 1DOF monolithic piezoactuator (MPA)". *Proceedings of SPIE Microrobotics and Microassembly III*, Vol. 4568, Newton – USA, pp. 151-162.
- Rodriguez-Fortun J.M., Orus J., Alfonso J., Buil F., 2011. "Hysteresis in Piezoelectric Actuators: Modeling and Compensation". Grupo de Investigación Aplicada (GIA-MDPI), Instituto Tecnológico de Aragón, Zaragoza, Spain. Instituto de Investigación en Ingeniería de Aragón (I3A), Universidad de Zaragoza, Spain.  
<<http://www.nt.ntnu.no/users/skoge/prost/proceedings/ifac11-proceedings/data/html/papers/1063.pdf>>
- Vautier B.J.G., Moheimani S.O.R., 2005. "Charge driven piezoelectric actuators for structural vibration control: issues and implementation". School of Electrical Engineering and Computer Science. University of Newcastle, Callaghan 2308, NSW, Australia <<http://routh.newcastle.edu.au/lab/pdf/J05d.pdf>>.

## 9. RESPONSIBILITY NOTICE

The authors are the only responsible for the printed material included in this paper.